Terahertz surface emission from $Cu_2ZnSnSe_4$ thin film photovoltaic material excited by femtosecond laser pulses

Zhenyu Zhao[1, a)], Gudrun Niehues[2], Stefan Funkner[2], Elmer Estacio[2, 3, b)], Qifeng Han[1], Kohji Yamamoto[2], Jingtao Zhang[1], Wangzhou Shi[1], Qixin Guo[1, 4], and Masahiko Tani[2, c)]

[1]Department of Physics, Shanghai Normal University, Shanghai 200234, China

[2]Research Center for Development of Far-Infrared Region, University of Fukui, Fukui 910-8507, Japan

[3] National Institute of Physics, University of the Philippines, Diliman, Quezon City, Philippines 1101

[4]Department of Electrical and Electronic Engineering, Saga University, Saga 840-8502, Japan

Z. Zhao, G. Niehues, S. Funkner, E. Estacio, Q. Han, K. Yamamoto, J. Zhang, W. Shi, Q. Guo, and M. Tani, "Terahertz surface emission from Cu2ZnSnSe4 thin film photovoltaic material excited by femtosecond laser pulses", Appl. Phys. Lett., 105, 231104 (2014)

and may be found at:
http://http://scitation.aip.org/content/aip/journal/apl/105/23/10.1063/1.4903740

[a)] Electronic mail: zyzhao@shnu.edu.cn
[b)] As visiting fellow. Permanent affiliation: National Institute of Physics, University of the Philippines Diliman
[c)] Electronic mail: tani@fir.u-fukui.ac.jp

Abstract

We observed efficient terahertz (THz) emission from sol-gel grown $Cu_2ZnSnSe_4$ (CZTSe) thin films using THz time domain spectroscopy technique. The THz emission bandwidth exceeds 2 THz with a dynamic range of 20 dB in the amplitude spectrum. The THz emission amplitude from CZTSe is found to be independent of external magnetic fields. Comparing the polarity of THz emission waveforms of CZTSe and GaAs, we suggest that the acceleration of photo-carriers in the surface accumulation layer of CZTSe is the dominant mechanism of radiation emission. Optical excitation fluence dependence measurements show that the saturation fluence of the CZTSe thin film reaches 1.48 $\mu J/cm^2$.

To date, most THz surface emitters for spectroscopy and imaging applications are based on the III-V semiconductor compounds, such as InP, InAs, GaAs, GaSb and InSb.[1-6] These materials are grown either by single-crystal growth processes or by thin film epitaxy methods,[7,8] which require stringent operating environments; while exhibiting extremely low growth rates. Alternatively, some photovoltaic materials (PV), such as black silicon and copper indium gallium selenide (CIGSe),[9,10] have been found to be efficient and low cost terahertz (THz) emitters due to their inherent electrical properties and cost-effective fabrication processes. Copper zinc tin selenide (CZTSe) is recognized as an alternative to CIGSe photovoltaic material due to the mineral abundance of zinc and tin, as well as its high degree of similarity to the electronic configuration of CIGSe.[11-13] Furthermore, CZTSe can be successfully fabricated in sol-gel processes; thereby reducing production costs and making it feasible in coating large areas.[14,15] Hence, sol-gel grown CZTSe may be considered as a promising and cost-effective PV material, as well as a radiation source for THz applications.

In this paper, we report the observation of efficient THz radiation from a surface-illuminated CZTSe thin film grown on soda-lime glass. The THz waveform is measured using a standard THz time domain spectroscopy (THz-TDS) technique. In addition to the structural and electrical characterization, the mechanism of the THz emission from CZTSe thin film is also investigated.

A 1 μm thick CZTSe thin film was grown on a 10 mm ×10 mm rectangular soda-lime glass substrate. The process route of CZTSe film growth is described in an earlier published work[15]. The structure of the as-grown CZTSe film was initially characterized by X-ray energy dispersive spectroscopy (EDS) and X-ray diffraction (XRD). The EDS measurement shows an extremely low sulfur content (S/(S+Se) = 0.04) of the as-grown CZTSe film indicating sufficient

substitution of sulfur by selenium. Furthermore, the stoichiometric composition of the as-grown CZTSe is Cu/(Zn+Sn) = 0.81 and Zn/Sn = 1.20. Fig. 1(a) shows the XRD curve of the CZTSe film. The three prominent Bragg diffraction angles appearing at 2θ = 27.6°, 45.5°, and 53.9°, are ascribed to the polycrystalline orientation (112), (204), and (116) correspondingly.[15,16] Fig. 1(b) shows the optical transmittance of as-grown CZTSe film, which is measured by a Cary-500 UV-NIR spectrophotometer. The inset depicts a fit by the Tauc plot method[13,17] yielding an optical bandgap (E_g) of 0.9 eV. It must be noted that the bandgap energy of CZTSe varies over a certain range, depending on the preparation parameters.[12-17] For this particular sample, the 0.9 eV bandgap ensures that the 800 nm-wavelength ($h\nu$ = 1.55 eV) optical excitation laser has sufficient photon energy to generate photocarriers at the CZTSe surface. The electrical properties of the sample were measured using a Lakeshore 7500 Hall measurement system at room temperature. The as-grown CZTSe sample was placed in the center of the sample holder with 4 tungsten needle probes in contact with the CZTSe at 4 right-angle corners of the sample in a standard van der Pauw configuration. The applied magnetic field is varied from –5000 G to +5000 G at a step rate of 500 G. It is found that the bulk carrier density of CZTSe reaches $3.7\times10^{18}/cm^3$ and a conductivity value of 8.3 S/cm. As a p-type material, the hole mobility of the as-grown CZTSe film, however, is only 14 cm^2/ V/s.

THz-TDS setup is shown in Fig. 2. A mode-locked Ti: sapphire laser (Spectra-Physics Tsunami) was used as the optical excitation source (central wavelength 800 nm, 80 fs pulses, 82 MHz repetition rate) to excite the surface of CZTSe thin film in a 45° incident-angle geometry. A lens with focal length of 500 mm was used to focus the beam to a relatively large spot of about 3 mm^2. The THz emission at the specular reflection direction was collimated and focused using two off-axis paraboloid reflectors onto a photoconductive dipole antenna on a low-temperature-

grown GaAs (LT-GaAs) substrate. The temporal window of each measurement is 40 ps with a time resolution of 2/3 ps. The time constant of the lock-in-amplifier-based signal acquisition is set to 100 ms. A surface-irradiated InAs wafer was used as a reference emitter to compare the THz-TDS waveform polarity from the CZTSe thin film under a magnetic field (B = 0, ±6500 G, the sign +/– refers to the magnetic field polarity). The magnetic field was oriented parallel to the sample surface. In addition, p-type GaAs (*p*-GaAs) and n-type GaAs (*n*-GaAs) wafers were used as reference emitters to compare the polarity of their THz radiation with the CZTSe thin film to possibly identify the direction of the conduction and valence band bending at the surface.

Figure 3(a) shows the THz emission waveforms from the CZTSe thin film. The corresponding THz emission amplitude spectra are presented in Fig. 3(b). The radiation bandwidth of the CZTSe emission exceeds 2 THz bandwidth, having a 20 dB dynamic range in the amplitude spectrum. Under the same excitation conditions, the intensity of the THz emission from CZTSe exceeds that of *p*-GaAs and is comparable to *n*-GaAs. The incident laser pulses are unable to penetrate deep into the CZTSe thin film due to the strong absorption in CZTSe ($\alpha > 6\times10^4$ cm^{-1} at 800 nm)[18]. As such, the emitted radiation is inferred to originate from the CZTSe surface rather than CZTSe/glass-substrate interface.

The THz surface emission in semiconductor materials is generally attributed to three mechanisms: [19] Optical rectification (OR), photo-Dember effect, and surface depletion field. The OR mechanism occurs only for highly oriented single crystals. Thus, OR can be initially excluded due to the polycrystalline structure of as-grown CZTSe thin film used in our study. The photo-Dember effect occurs only when the photo-excitation energy exceeds the bandgap of the material by a large value and the semiconductors must be of high electron mobility, (i.e. $\mu > 10^4$ $cm^2/V/s$). This effect originates from ultra-fast photo-generation of charge carriers and

subsequent carrier diffusion, inducing a charge dipole in the vicinity of a semiconductor surface owing to the difference of the mobilities (or diffusion constants) for holes and electrons; leading to an effective charge separation in the direction perpendicular to the surface. The induced dipole oscillation causes a distinct THz surface emission. In order to investigate the role of the photo-Dember effect in the THz emission mechanism of CZTSe, we compare the influence of the B-field polarity applied parallel to the sample surface on the THz waveforms emitted by CZTSe and InAs. The magnetic field induces a Lorenz force to the diffusing carriers affecting the direction of the carrier separation. The THz waveforms of CZTSe and InAs under different magnetic field directions are shown in Fig. 4. The THz emission waveform from InAs is significantly affected by the polarity flipping of the applied B field. However, that of the CZTSe sample remained unchanged by the B field; indicating that the diffusion velocity of carriers in CZTSe is low and/or the effective mass of the carrier is large. Furthermore, InAs is a well-known photo-Dember material of high electron mobility $\mu = 3\times10^4$ $cm^2/V/s$, with magnitude 3 orders higher than that of CZTSe (μ=14 $cm^2/V/s$). This sharp contrast between the THz emission characteristics dependence on an external B field further supports the inference that the photo-Dember effect cannot be the dominant THz emission process for CZTSe; even as its contribution cannot completely excluded.

The last plausible THz emission mechanism is the photo-excited transient surge current at the surface of CZTSe films. Normally, a space charge region exists in extrinsic semiconductors due to the Femi-level pinning and band bending at the surface region.[20] The photo-generated carriers at the semiconductor surface are accelerated by the depletion field in the space charge region, causing a surge current transient that is normal to the surface. This transient drift current generates detectable THz-frequency electromagnetic pulses. The direction of the band bending at

the surface depends on the type of the major dopant: either *n*-type or *p*-type. The energy bands bend upward in *n*-GaAs and downwards in its *p*-doped counterpart.[19] Consequently, the surge current direction of *p*-type semiconductor is opposite that of its *n*-type counterpart. Figure 3 shows that *n*-GaAs exhibits a distinct valley-to-peak THz waveform, while the *p*-GaAs exhibit a peak-to-valley waveform. The observed THz polarity of CZTSe is the same as that of *n*-GaAs. This initially indicates that the surface band structure of CZTSe bends upward even though CZTSe is intrinsically p-type.

A proposed explanation for this result is based on the possible existence of an accumulation layer in the CZTSe film. If a semiconductor surface is highly *p*-type, the edge of valence band is very close to the Fermi-level near the surface. For upward band bending, negative surface charges exist; allowing holes to accumulate at the CZTSe surface. This causes the formation of an accumulation layer rather than a depletion layer. The direction of the band bending of an accumulation layer of a *p*-type semiconductor is similar to that of the depletion layer in an *n*-type semiconductor.[20] The diagram of surface band bending of semiconductor as well as the polarity of emitted THz radiation is illustrated in Fig. 5. The carrier concentration at the surface is above the bulk value, thus leading to a surface accumulation.[20] Van der Pauw measurements show that the bulk carrier density of CZTSe reaches $3.7\times10^{18}/cm^3$, which is sufficient to cause an accumulation layer at the surface of CZTSe. Therefore, it is proposed that the surface band bending in strongly *p*-type CZTSe is upward owing to the presence of an accumulation layer, causing the THz emission polarity to be the same as that of the *n*-GaAs reference emitter. Even though the photo-Dember effect cannot be totally excluded from the possible THz radiation mechanism owing to the absence of differently-doped CZTSe samples for comparison, the current experimental results strongly suggest that the acceleration of

photocarriers by the built-in field established by the surface accumulation layer in CZTSe is the dominant THz radiation mechanism.

Finally, the THz emission efficiency of as-grown CZTSe thin film is evaluated by an excitation fluence-dependence measurement. Normally, the electrical field amplitude of photo-carriers acceleration induced THz surface emission is proportional to the time-derivative of the surge current:[19,21)]

$$E_{THz} \propto \frac{\partial J}{\partial t} \propto \frac{\partial}{\partial t}(nq\mu \times E) \propto \frac{\partial}{\partial t}(\sigma \times E), \quad (1)$$

where J is surge current density, n is the number density of photo-carriers, q is the electron charge, μ is the carrier mobility, σ is the conductivity, and E is the driving electric field. Equation (1) shows that an incident light having a higher intensity will result in a stronger THz emission owing to a higher density of photo-carriers. However, a sufficiently high charge density of photo-carriers will rapidly screen out the built-in field at the surface of the CZTSe film; resulting in the saturation of the THz emission [19)]. The fluence dependence of the THz emission from the CZTSe film is presented in Fig. 6. The experimental plots were fitted with the following formula:[19)]

$$E_{THz} = \frac{E_0}{1 + F_{sat}/F}, \quad (2)$$

where, the E_{THz} is the amplitude of THz radiation, E_0 is the THz amplitude in the high fluence limit, F is the optical fluence, F_{sat} is the saturation fluence at which the THz amplitude reaches the half of E_0. By fitting Eq. (2) to the experimental data, we obtained F_{sat} = 1.48 μJ/cm^2. For the GaAs reference, however, such a saturation behavior was not distinctly observed. However, an earlier published work reported that the saturation fluence for GaAs can be as high as F_{sat} = 9.6 μJ/cm^2; which exceeds the specifications of the optical excitation used in our THz-TDS setup[22)].

The relatively lower F_{sat} of CZTSe can be attributed to the strong absorption ($\alpha > 6\times10^4$ cm^{-1} at 800 nm)[18], which is higher than that of GaAs ($\alpha \sim 1\times10^4$ cm^{-1} at 800 nm) [23], and a relatively longer carrier lifetime; up to nanosecond regime,[24,25] both of which increase the photocarrier density on the CZTSe surface.

In summary, we observed efficient THz surface emission from a CZTSe thin film excited by a femtosecond laser. It is found that the THz emission of the CZTSe film appears to be independent of the external magnetic field. From the polarity of THz waveform relative to that from *p*-GaAs and *n*-GaAs, the mechanism of THz generation from the CZTSe thin film is suggested to be due to the acceleration of photo-carriers in accumulation layer of the CZTSe. Optical excitation fluence dependence measurement shows that the saturation fluence of CZTSe thin film reaches 1.48 μJ/cm^2.

Acknowledgements

This work was financially supported by the National Natural Science Foundation of China (Grant No. 61307130, 61376010 and 61475168) as well as the Innovation Program of Shanghai Municipal Education Commission (Grant No.14YZ077). ZZ gratefully acknowledges the Scientific Research Foundation for the Returned Overseas Chinese Scholars, State Education Ministry. SF and GN gratefully acknowledge the Japan Society for the Promotion of Science (JSPS) and the Alexander von Humboldt Foundation for supporting their work through postdoctoral fellowships.

References

1. M. B. Johnston, D.M. Whittaker, A. Corchia, A.G. Davies, E. H. Linfield, *Phys. Rev. B* **65**, 165301 (2002)
2. R. Ascázubi, I. Wilke, K. Denniston, H. Lu, and W.J. Schaff, *Appl. Phys. Lett.* **84**, 4810 (2004).
3. R. Ascázubi, C. Shneider, I. Wilke, R. Pino, and P. S. Dutta, *Phys. Rev. B* **72**, 045328 (2005).
4. R. Ascázubi, I. Wilke, K. J. Kim, and P. Dutta, *Phys. Rev. B* **74**, 075323 (2006).
5. L. M. Vitalij, A. Ramunas, and K. Arunas, *C. R. Physique* **9**, 130 (2008).
6. S. L. Dexheimer (Ed.), Terahertz Spectroscopy: Principles and Applications, (CRC, 2008).
7. P. S. Dutta (Ed.), Springer Handbook of Crystal Growth, (Spring Verlag, Berlin, 2010), pp 281-325.
8. R. C. Jaeger (Ed.), Introduction to Microelectronic Fabrication (2nd ed.), (Prentice Hall, 2002), pp 129-150.
9. P. Hoyer, M. Theuer, R. Beigang, and E.-B. Kley, *Appl. Phys. Lett.* **93**, 091106 (2008).
10. R. Adomavičius, A. Krotkus, J. Kois, S. Bereznev, and E. Mellikov, *Appl. Phys. Lett.* **87**, 191104 (2005).
11. T. K. Todorov, K. B. Reuter, and D. B. Mitzi, *Adv. Mater.* **22**, E156 (2010).
12. F. Luckert, D. I. Hamilton, M. V. Yakushev, N. S. Beattie, G. Zoppi, M. Moynihan, I. Forbers, A. V. Karotki, A. V. Mudryi, M. Grossberg, J. Krustok, and R. W. Martin, *Appl. Phys. Lett.* **99,** 062104 (2011).
13. S. Ahn, S. Jung, J. Gwak, A. Cho, K. Shin, K. Yoon, D. Park, H. Cheong, and J. H. Yun, *Appl. Phys. Lett.* **97**, 021905 (2011).
14. J. V. Li, D. Kuciauskas, M. R. Young, and I. L. Repins, *Appl. Phys. Lett.* **102**, 163905 (2013).

15. Y. Li, Q. Han, T.-W. Kim, and W. Shi, *J. Sol-Gel Sci. Technol.* **69**, 260 (2014).

16. Y. Liu, D. Kong, H. You, C.Chen, X. Lin, and J. Brugger, *J. Mater. Sci: Mater. Electron.* **24**, 529 (2013).

17. O. Stenzel (Ed.), The Physics of Thin Film Optical Spectra: An Introduction (Spring Verlag, Berlin 2005), p. 214.

18. C. Perssona, *J. Appl. Phys.* **107**, 053710 (2010).

19. K. Sakai (Ed.), Terahertz Optoelectronics (Spring Verlag, Berlin 2005), p. 63-76.

20. W. Mönch (Ed.), Semiconductor Surfaces and Interfaces (Spring Verlag, Berlin 1993), p. 24-25.

21. H. Nakanishi, S. Fujiwara, K. Takayama, I. Kawayama, H. Murakami, and M. Tonouchi, *Appl. Phys. Express.* **5**, 112301 (2012).

22. M. Reid and R. Fedosejevs, *Appl. Opt.* **44,** 149 (2005).

23. H. C. Casey, D. D. Sell, and K. W.Wecht, *J. Appl. Phys.* **46**, 250 (1975).

24. O. Gunawan, T. K. Todorov, and D. B. Mitzi, *Appl. Phys. Lett.* **97**, 233506 (2010).

25. B. Shin, Y. Zhu, N. A. Bojarczuk, S. Jay Chey, and S. Guha, *Appl. Phys. Lett.* **101**, 053903 (2012).

Figures Captions

Fig. 1. (a): XRD data of CZTSe. (b) Optical transmittance of CZTSe; Inset: Tauc plot of the transmittance (E_g=0.9 eV), of which the y-axis refers to $(\alpha hv)^2$. Dot line: Fitted optical bandgap.

Fig. 2. The schematic setup of THz-emission time-domain spectroscopy.

Fig. 3. (a):THz waveform of CZTSe; (b): THz waveform of *n*-GaAs; (c): THz waveform of *p*-GaAs. (d): THz spectrum of CZTSe; (e): THz spectrum of *n*-GaAs; (f): THz spectrum of *p*-GaAs.

Fig. 4. THz emission waveforms of CZTSe and InAs reference under different magnetic field. Red solid line: B=0, Green solid line: B=+6500 G, Blue solid line: B= –6500 G. The Graph (a), (b), and (c) refer to the THz waveforms of CZTSe film, The Graph (d), (e), and (f) refer to the THz waveforms of InAs reference.

Fig. 5. Diagram of the relation between THz polarity and the surface band bending of extrinsic GaAs as well as CZTSe thin film.

Fig. 6. THz amplitude as a function of incident optical fluence. Solid spheres: THz amplitude of CZTSe. Solid line: Fitting curve corresponding to the sample.

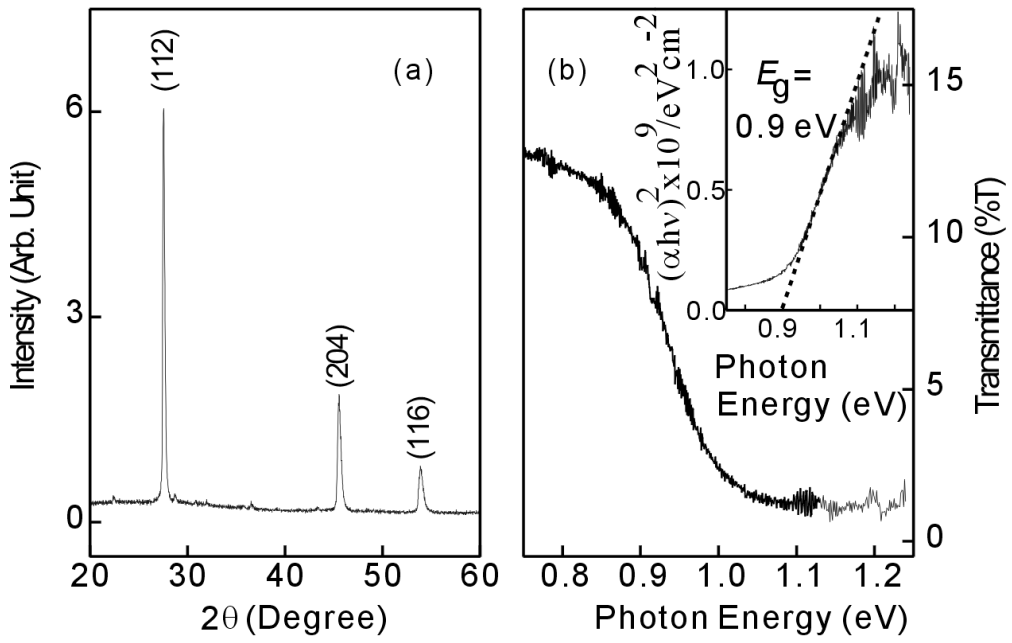
(a)
(112)
(204)
(116)
Intensity (Arb. Unit)
2θ (Degree)
(b)
E_g = 0.9 eV
$(\alpha h\nu)^2 x10^9 /eV^2 cm^{-2}$
Photon Energy (eV)
Transmittance (%T)

FIG. 1.

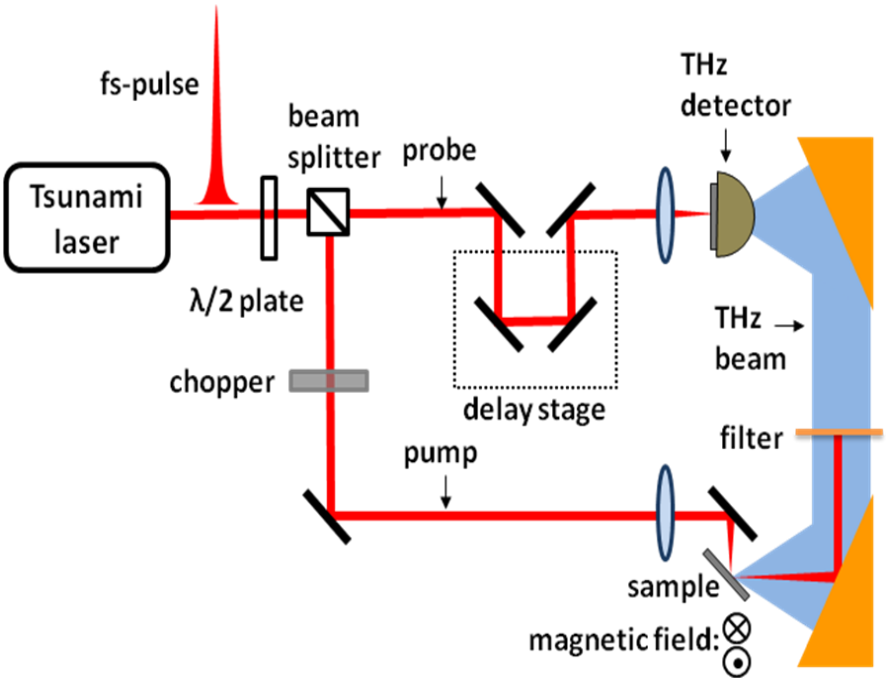
fs-pulse
beam splitter
probe
THz detector
Tsunami laser
λ/2 plate
chopper
delay stage
THz beam
filter
pump
sample
magnetic field:

FIG. 2.

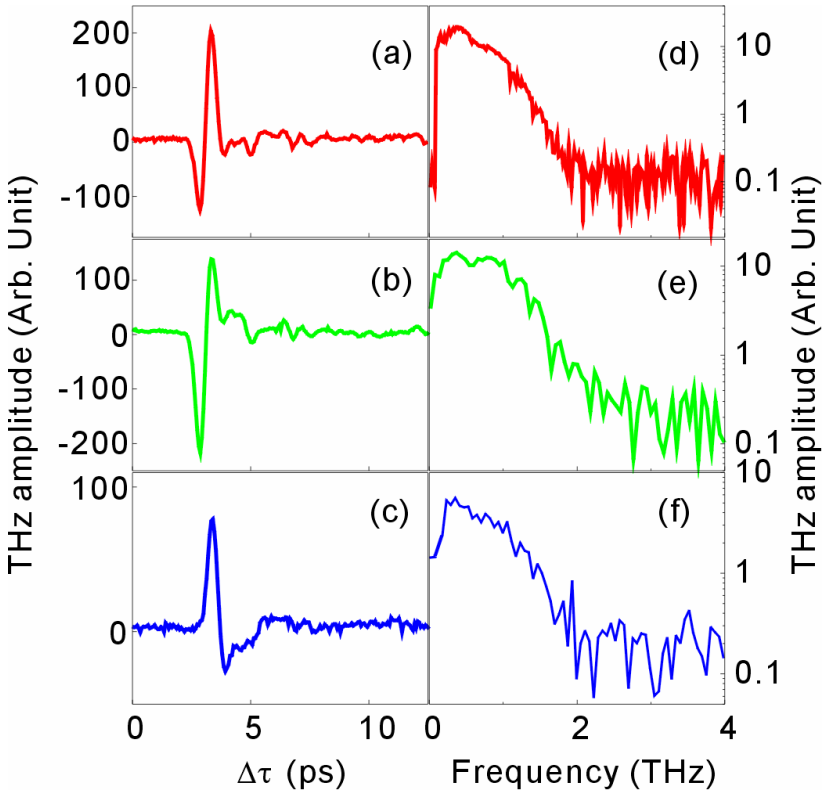
(a)
(b)
(c)
(d)
(e)
(f)
THz amplitude (Arb. Unit)
THz amplitude (Arb. Unit)
Δτ (ps)
Frequency (THz)

FIG. 3.

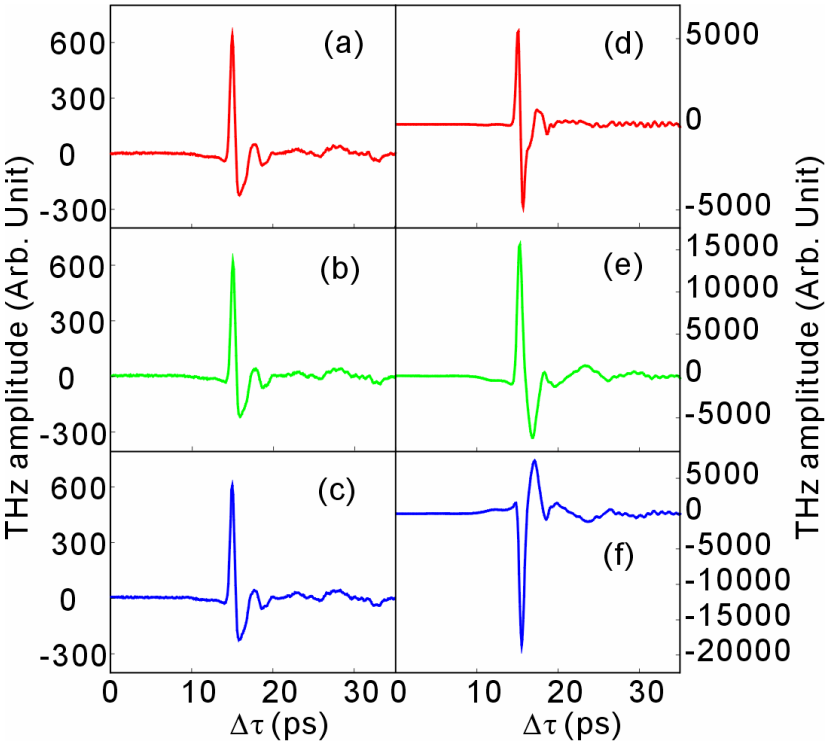
(a)
(b)
(c)
(d)
(e)
(f)
THz amplitude (Arb. Unit)
THz amplitude (Arb. Unit)
Δτ (ps)
Δτ (ps)

FIG. 4.

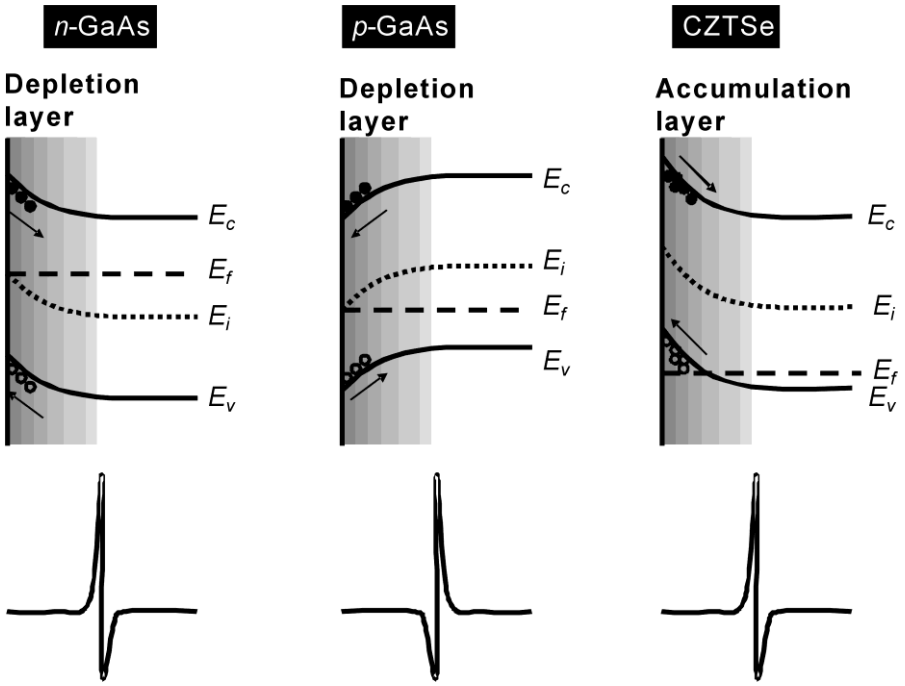
n-GaAs
p-GaAs
CZTSe
Depletion layer
Depletion layer
Accumulation layer
E_c
E_f
E_i
E_v

FIG. 5.

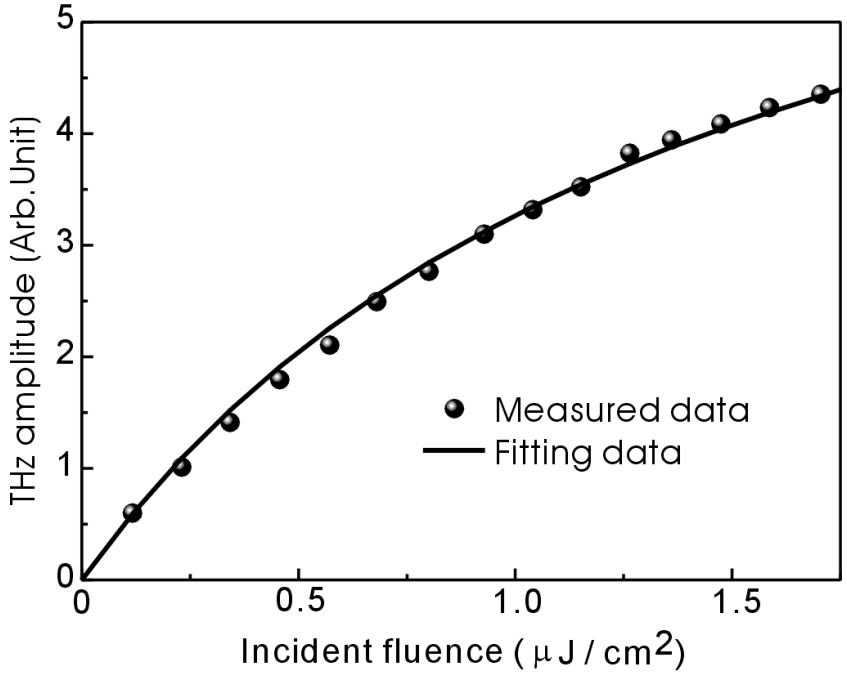
THz amplitude (Arb.Unit)
Incident fluence (μJ / cm2)
Measured data
Fitting data
0
1
2
3
4
5
0
0.5
1.0
1.5

FIG. 6.